

Decomposition of Substituted Alkoxy radicals - Part I:  
A Generalized Structure-Activity Relationship for reaction barrier heights

— Supporting Information —

L. Vereecken,\* J. Peeters

Department of Chemistry, K.U.Leuven, Celestijnenlaan 200F, B-3001 Leuven, Belgium

**Table of content**

- p. 2: Curvature at low barrier heights
- p. 3: Quantum chemical calculations
- p. 7: Substituents and functionalities
- p. 15: Statistical analysis of the fitting procedure
- p. 17: SAR parameters in  $\text{kJ mol}^{-1}$

### Curvature at low barrier heights: Linear prediction model versus the B3LYP $E_b$ :

Predicting the B3LYP barrier heights  $E_b$  using a linear model based on the number of substituents works quite well for barriers above 7 kcal/mol, with a fairly well behaved linear additivity and comparatively little scatter (see figure SI-3).

For highly substituted compounds however, the linear SAR can predict negative barrier heights when the sum of the activities over all substituents  $\sum F_s \times N(s)$  is higher than the value  $E_b(\text{CH}_3\text{CH}_2\text{O}^\bullet)$ . As the true barrier height, as calculated using B3LYP, can not be negative, this will cause a discrepancy between the linear SAR prediction and the B3LYP data. We find that for barriers below 5 to 7 kcal/mol as calculated using B3LYP, the linear SAR already starts to deviate from the B3LYP data (see figure SI-3). This can be corrected for by correcting the linear SAR for the curvature towards  $E_b=0$  kcal/mol of the B3LYP data. The functional form of this correction is mostly arbitrary, and a Gaussian curve was found to work well (see main text). After transformation by this function, the SAR predictions  $E_b(\text{SAR})$  are again close to the B3LYP data (see Figure SI-3 and SI-4).

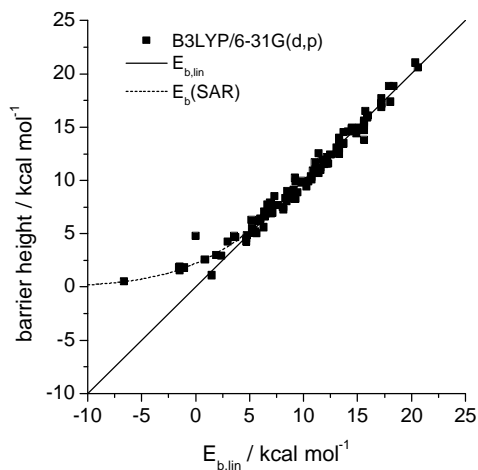


**Fig. SI-3:** Comparison of the SAR predictions versus the B3LYP-calculated barriers. The diagonal line indicates perfect agreement between the linear SAR  $E_{b,\text{lin}}$  and B3LYP barrier heights. The dotted curved line represents the SAR predictions  $E_b(\text{SAR})$  after curvature correction of the linear  $E_{b,\text{lin}}$ .

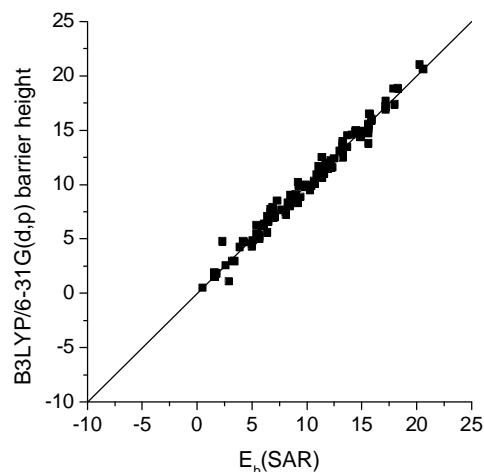


**Fig. SI-4:** Comparison of the SAR predictions  $E_b(\text{SAR})$  after curvature correction, versus the B3LYP-calculated barriers. The diagonal line indicates perfect agreement.

## Quantum chemical calculations

The barrier heights for dissociation were obtained by full optimization of all of the conformers of the reactant, and of the transition states for dissociation, at the chosen level of theory. The intrinsic barrier height  $E_b$  for dissociation is then defined as the energy difference, after ZPE-correction, between the most stable conformer of the reactant, and the lowest-lying conformer of the TS for the decomposition under consideration. It must be understood that the barrier height defined thus, i.e. the relative energy of the geometry with the highest energy along the minimum energy path from reactant to product in an elementary reaction, ensures that the barrier height is always  $\geq 0$  kcal mol<sup>-1</sup>. For barrierless decompositions, the use of barrier heights  $E_b$  may become less appropriate, and the entropic kinetic bottleneck should be used instead; this may be located at a geometry below the reactant energy level, leading to negative Arrhenius activation energies  $E_A$ .

Due to the large number of calculations involved –over 1500 conformers of over 200 structures are considered in this study– we chose to initially use methodologies that are of a reasonable computational cost, i.e. density functional theory and MP2, using a variety of basis sets. Higher-level calculations involving explicit correlation and/or extrapolation schemes are in progress, but due to their computational expense insufficient data is yet available to obtain a SAR on a sufficiently wide range of functionalities. Higher-level results are also available for some reactions in the literature (see e.g. the data listed in ref. 1). However, using an inconsistent set of calculations at different levels of theory obfuscates the reactivity trends we try to capture in the SAR, and we prefer to derive the SAR based on data at a single level of theory only.

The levels of theory used here are: B3LYP-DFT<sup>2,3</sup> with the 6-31G(d,p) (5d orbitals), 6-311++G(2df,2pd), and aug-cc-pVTZ basis sets, BB1K-DFT<sup>4</sup> with the 6-31+G(d) basis set, MPW1K-DFT<sup>5</sup> with the 6-31G(d,p) and 6-311++G(2df,2pd) basis sets, MPWKIS1K-DFT<sup>6</sup> with the 6-31+G(d,p) and 6-311++G(2df,2pd) basis sets, and MP2 with the 6-31G(d,p) (6d orbitals) basis set. Additionally, CBS-QB3<sup>7</sup> benchmark calculations were performed on the most stable conformers of a selected subset of compounds and transition states. All calculations were performed using the Gaussian-98<sup>8</sup> and Gaussian-03<sup>9</sup> quantum chemical software.

Table 1 in the main paper compares the barrier heights obtained at these levels of theory against the experiment-derived data and the CBS-QB3 high-level results. A first trend apparent from these results is that the DFT results are sensitive to the basis set selected: larger basis sets yield a systematically lower barrier height for decomposition. We reported this trend earlier for the B3LYP functional,<sup>1,10</sup> but the tendency holds for all DFT functionals used here. A second observation is that many levels of theory overestimate the barrier heights, by several kcal mol<sup>-1</sup>, making them irreconcilable with the experimental data or the CBS-QB3 data. The level of theory used in our earlier work,<sup>1</sup> B3LYP/6-31G(d,p), shows the best performance in this respect, usually reproducing the experimental and CBS-QB3 barrier heights within  $\pm 1$  kcal mol<sup>-1</sup>. That study also showed that the B3LYP/6-31G(d,p) level of theory is also in good agreement with other higher-level calculations, including G2(MP2), Coupled-Cluster, and CBS-RAD. A notable exception to the good agreement with CBS-QB3 is for the acetonoxo radical (CH<sub>3</sub>C(O)CH<sub>2</sub>O<sup>•</sup>); this was described earlier also for G2 and G3 calculations,<sup>10</sup> and is caused by an unusual sensitivity of the geometry to the basis set used in MP2 calculations, invalidating the MP2 basis set extrapolation step used in these higher-level methodologies, as shown in the figure SI-5:

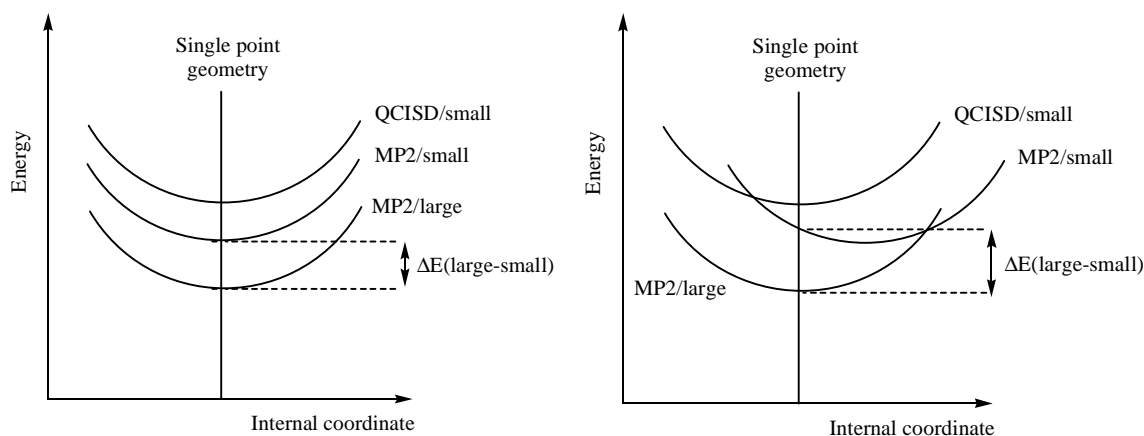


**Fig. SI-5:** Depiction of the extrapolation scheme to calculate QCISD/large energies for a single geometry from the QCISD/small energy as  $\text{QCISD/large} = \text{QCISD/small} + \Delta E(\text{large-small})$ , using the energy difference  $\Delta E(\text{large-small})$  between the small and large basis set obtained at the MP2 level of theory. **Right hand side:** the potential energy surfaces at all levels of theory are parallel, allowing correct calculation of the energy difference  $\Delta E(\text{large-small})$ . **Left hand side:** the potential energy surfaces at different levels of theory are significantly different, such that the energy difference  $\Delta E(\text{large-small})$  calculated not only reflects the energy change due to a difference in basis set, but also due to a difference in PES topology.

The DFT functionals BB1K, MPW1K, and MPWKCIS1K all yield barriers higher than the experimental data by several kcal mol<sup>-1</sup>. Likewise, MP2 calculations systematically overestimate the barrier height by a wide margin. It is important to note that the overestimation is not a randomly distributed uncertainty, but rather introduces a systematic bias to all the barrier heights compared to the experimental data. All levels of theory used here show very similar trends in reactivity with varying substitution of the alkoxy radical. That the reactivity *trends* are reproduced faithfully, even if the absolute barrier heights are shifted relative to the reference data, indicates that the *change* in interactions are properly described at all these levels of theory. Hence, as the prime condition for our SAR development is a correct description of the relative change of the barriers, all levels of theory considered here can in principle be used to derive a SAR by shifting the predicted barrier heights up or down by a fixed value. Still, we select the B3LYP/6-31G(d,p) level of theory as the methodology of choice in this work, given that its absolute barrier heights are already in good agreement with experiment and higher level calculations.

The overestimation of the barrier height by the MP2 level of theory is not entirely unexpected: the level of correlation included in this methodology is insufficient for accurate energies, and the basis set used is comparatively small for methodologies using explicit electron correlation. The differences between the DFT functionals, and their dependencies on the basis set, were not expected to be so pronounced, especially considering that some of these functionals were explicitly developed for theoretical kinetic calculations. Apparently this reaction class has its specific peculiarities that are not fully accounted for in some of these methodologies. Similar systematic shifts are already documented, e.g. the tendency of B3LYP to underestimate barrier heights for bimolecular H-transfer reactions; these reactions are in turn better treated by the other functionals who contain several H-transfer reactions in their training set. It could be argued that relying on the B3LYP/6-31G(d,p) level of theory for the current SAR development relies too heavily on a fortuitous cancellation of error, giving apparently correct barrier heights for the wrong reasons, and hence being unreliable for barriers for which no experimental data for comparison is available. Here, we rely on the good agreement with the CBS-QB3 data, and the fact that all the levels of theory used in this work reproduce similar trends in reactivity as observed for B3LYP/6-31G(d,p). While

we have not characterized all molecules using all methodologies due to the computational expense, dozens of molecules were studied to verify this assertion. With numerous methodologies yielding the same trends, we have confidence that the dependence on the substitution as incorporated in the Structure-Activity Relationship is well characterized, while the absolute barrier heights are benchmarked for key species against the experimental and high-level theoretical values. Within the expected accuracy of the results, the SAR will then be useful in the prediction of the (relative) rates of reactions, especially as one reaction will often be found to strongly dominate the other channels, such that the uncertainty on the absolute rate has a minor impact. Extensive high-level theoretical calculations are in progress, generating a data set that in future work will be used to fine-tune the SAR.

### 3. Substituents and functionalities

Below, we discuss each of the substituents and functionalities investigated in this paper: alkyl ( $-R$ ), oxo ( $=O$ ), hydroxy ( $-OH$ ), alkoxy ( $-OR$ ), hydroperoxy ( $-OOH$ ), alkylperoxy ( $-OOR$ ), nitroso ( $-NO$ ), nitro, ( $-NO_2$ ), nitrosooxy ( $-ONO$ ), and nitroxy ( $-ONO_2$ ) substituents, as well as unsaturated functionalities ( $-C=C$ ,  $=C$ ) and some cyclic structures. This selection does not necessarily reflect their relative importance in atmospheric chemistry.

The available data indicates<sup>1,11</sup> that the decomposition rates are mostly affected by substitution around the  $\alpha$ - and  $\beta$ -carbons of the breaking C–C bond, where the impact of a particular substituent can differ notably<sup>1,12</sup> depending on which of the two pertaining carbons it is bonded to. We therefore focus on substituents on the  $\alpha$ - and  $\beta$ -carbons, except for unsaturated compounds where delocalization and conjugation effects over larger distances are important. Where appropriate, some other long-distance influences, e.g. H-bonding, are discussed.

#### 3.1 Alkyl substituents ( $-R$ )

The organic compounds emitted or formed in the atmosphere show a wide variety in their carbon skeleton. Experimental and theoretical evidence indicates that the presence of alkyl substituents on either of the  $\alpha$ - and  $\beta$ -carbons lowers the barrier height for decomposition.<sup>1,11,13</sup> The number of alkyl substituents on the  $\alpha$ - and  $\beta$ -carbons is the determining factor, while the length and branching of each of the alkyl substituents does not influence the barrier height significantly. Numerous examples of this are found in Table 2 in the main paper, including the systematic series of the 1-alkoxy and 2-alkoxy radicals. The absolute uncertainty on the available data is larger than the small relative differences that might be derived for specific, longer or branched alkyl substituents, so for the purpose of this SAR all saturated, non-cyclic (branched) alkyl substituents are lumped into a single substituent class.

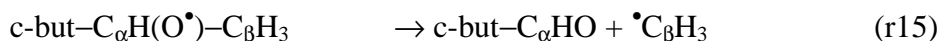
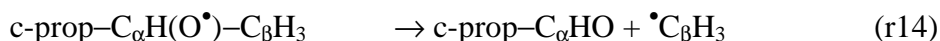
In principle, this lumping becomes invalid for alkyl side chains who themselves bear non-alkyl substituents close to the reaction site, as the specific interaction of these subgroups with the reaction site can affect the barrier heights. An important example in atmospheric chemistry is the presence of oxygen-bearing substituents near the breaking bond, where the strongly electronegative oxygen atom affects the electron density of the breaking bond prior to the reaction, and the newly formed carbonyl bond or the radical

site after the decomposition. The effect of oxygen-bearing functionalities, e.g. in the H-abstraction reaction by OH radicals, has been documented.<sup>14</sup> Table 2 shows several examples of alkoxy decomposition reactions with an oxygenated group Y within an alkyl substituent on the  $\alpha$ -carbon, where Y = -OR, -OOH, -OOR, =O, or -OH:



Here, the presence of additional electronegative oxygen atoms near the forming C=O carbonyl bond increases the alkoxy decomposition barrier height, on average by  $\sim 1.6$  kcal mol<sup>-1</sup> relative to the value expected for a  $-\text{C}_n\text{H}_{2n+1}$   $\alpha$ -alkyl group such as  $-\text{CH}_3$  or  $-\text{C}_2\text{H}_5$ . The effect is less pronounced,  $\sim 0.5$  kcal mol<sup>-1</sup>, for Y = -OH, due to partial compensation from the stronger H-bonding between the OH hydrogen and the carbonyl oxygen in the  $\text{H}_2\text{C}(\text{OH})-\text{C}_\alpha\text{HO}$  product, compared to the  $\text{H}_2\text{C}(\text{OH})-\text{C}_\alpha\text{H}(\text{O}^\bullet)-\text{C}_\beta\text{H}_3$  reactant. The increase in barrier height is related to the difficulty of charge migration from the alkyl H and C atoms to the more electronegative oxygen atoms in a very small carbonyl fragment, and is therefore expected to largely disappear when more or longer  $\alpha$ -alkyl substituents are present. An example in point is the 14.0 kcal mol<sup>-1</sup> barrier for  $\bullet\text{CH}_3$  elimination in  $\text{HC}(\text{O})\text{C}(\text{O}^\bullet)(\text{CH}_3)_2$ , which is nearly identical to the 13.9 kcal mol<sup>-1</sup> barrier in  $\text{CH}_3\text{C}(\text{O}^\bullet)(\text{CH}_3)_2$ ; the barrier for the smaller  $\text{HC}(\text{O})\text{CH}(\text{O}^\bullet)\text{CH}_3$ , 17.1 kcal mol<sup>-1</sup>, was still significantly higher than the  $\text{CH}_3\text{CH}(\text{O}^\bullet)\text{CH}_3$  barrier of 15.1 kcal mol<sup>-1</sup>. This trend was observed for all DFT functionals and basis sets examined. We attempt here to improve the predictive accuracy of the SAR by including a separate parameter for alkoxy radicals with a single oxygenated alkyl substituent on the  $\alpha$ -carbon of the types  $-\text{CH}_2\text{OR}$ ,  $-\text{CH}_2\text{OOR}$ ,  $-\text{CH}_2\text{OOH}$ , and  $-\text{CHO}$ . We have insufficient data to derive an analogous parameter for oxygenated alkyl substituents on the  $\beta$ -carbon.

A related issue is the presence of cyclic structures in the alkyl substituent. Even if neither the  $\alpha$ - or  $\beta$ -carbon are member of a cyclic structure, the specific demands on the orbital arrangement in small, highly strained ring structures such as cyclopropyl (c-prop) and cyclobutyl (c-but) affects the interaction with the neighboring atoms compared to e.g. an unstrained isopropyl substituent:



Even small changes in ring strain or hyperconjugation interaction is likely to affect the barrier heights. For the reactions shown above, we find that the calculated barrier to decomposition is lower than expected for a regular  $C_\alpha$  alkyl substituent such as  $-\text{CH}_3$ . Not surprisingly, the effect is most pronounced for cyclopropyl, with a  $1.8 \text{ kcal mol}^{-1}$  lowering for the formation of *c*-prop-CHO in the reaction above, compared to methyl elimination in  $(\text{CH}_3)_2\text{CH}-\text{CH}(\text{O}^\bullet)-\text{CH}_3$ . For cyclobutyl, at  $0.9 \text{ kcal mol}^{-1}$ , the effect is already much less; in 5-membered and larger rings, we expect the effect to be mostly negligible. At this time, we prefer not to include a specific parameter in the SAR to account for this, as it is probably rarely needed, and furthermore is expected to depend on additional substitutions on the ring structure. Compounds where either or both of  $C_\alpha$  and  $C_\beta$  are themselves part of a cycle are discussed below.

### 3.2 Oxo substituents (=O)

The atmospheric oxidation of large biogenic hydrocarbons such as the terpenes has a tendency to form stable, partially oxidized hydrocarbons as intermediates, often bearing carbonyl functionalities. These oxygenates play a pivotal role in atmospheric chemistry, where their role in the formation of secondary organic aerosols receives a lot of attention. The atmospheric oxidation of such carbonyl-substituted oxygenates readily leads to oxo-substituted alkoxy radicals. Oxo-substitution on the  $\beta$ -carbon results in a substantial lowering of the barrier height,<sup>1</sup> owing to the stability of the acyl product radical,  $-\text{C}^\bullet=\text{O}$ . While the DFT geometries are generally insensitive to the basis set, the MP2 results for  $\beta$ -oxo-alkoxy radicals can be strongly dependent on the basis set used,<sup>10</sup> in particular with regard to the  $^\bullet\text{O}-\text{C}-\text{C}=\text{O}$  dihedral angle. This also affects basis set extrapolation schemes at the MP2 level of theory often used in compound single point energy calculations, see e.g. ref 10 or the CBS-QB3 result for acetonoxyl listed in Table 1 of the main paper.

With an oxo-substituent present directly on the  $\alpha$ -carbon, decomposition of the alkoxy radical leads to  $\text{CO}_2$  as co-product; this decomposition is strongly exothermic, resulting in a very pronounced lowering of the decomposition barrier. The quantum chemical characterization of the transition states for these reactions is complex, owing to the presence of multiple accessible electronic surfaces. While a complete analysis is outside the scope of this article, a short discussion of this aspect here is in order. As described in the literature, acyloxyl radicals,  $\text{R}-\text{C}(\text{O})\text{O}^\bullet$ , have several electronic states within a few

kcal mol<sup>-1</sup> of the ground state, e.g. the HC(O)O<sup>•</sup> shows the <sup>2</sup>A<sub>1</sub> and <sup>2</sup>A' low-lying electronic states within 3 kcal mol<sup>-1</sup> of the <sup>2</sup>B<sub>2</sub> ground state,<sup>15</sup> and the CH<sub>3</sub>C(O)O<sup>•</sup> radical has a <sup>2</sup>A' state less than 6 kcal mol<sup>-1</sup> above the <sup>2</sup>A'' ground state,<sup>16</sup>. A more detailed analysis of the CO<sub>2</sub> elimination in the larger CH<sub>3</sub>CH<sub>2</sub>C(O)O<sup>•</sup> radical shows two potential energy surfaces, geometrically differing mainly in the O–C–O angle, and the O–C–C–C dihedral angle. A first surface is characterized by an O–C–O angle of ~114° at longer elongation of the breaking C–C bond, probably correlating to a higher-energy conformer of the CO<sub>2</sub> product.<sup>17</sup> Using the B3LYP-DFT level of theory, we were unable to fully characterize this surface as the calculations collapsed to the second, lower surface at C–C bond elongation beyond 2 Å. At about 1.9 Å separation, the preferred orientation of the CO<sub>2</sub> moiety on the first surface is still in the C–C–C plane of symmetry, as it is in the CH<sub>3</sub>CH<sub>2</sub>C(O)O<sup>•</sup> reactant. The relative energy at this separation is ~22 kcal mol<sup>-1</sup> above the reactant and is therefore energetically not accessible as dissociation channel; rotation of the CO<sub>2</sub> moiety along the breaking C–C bond requires about 1.5 kcal mol<sup>-1</sup>. A second surface, showing an increasing O–C–O angle at larger separation, ultimately correlates to the linear CO<sub>2</sub> product ground state. The preferred orientation of the CO<sub>2</sub> moiety during the dissociation is approximately 45° relative to the C–C–C plane at C–C separations of 1.6 Å and beyond, i.e. different from the in-plane orientation in the reactant, with a C–C bond length of 1.5 Å. The surface at a C–C bond length of about 1.6 Å has an energy of 3.3 kcal mol<sup>-1</sup> above the reactants, and smoothly decreases in energy towards larger separations, with an energy of 1.1 kcal mol<sup>-1</sup> at a 1.9 Å separation. With two potential energy surfaces in close proximity at the relevant fragment separation, the characterization of the decomposition TS is difficult, especially considering that we used only single-reference methodologies in this work. Energy extrapolation schemes such as the Gaussian Gx or CBS families are likewise suspected to suffer from reduced accuracy. An in-depth investigation using high-level, preferably multi-reference, methodologies is needed to fully elucidate this matter. However, irrespective of the difficulties at short separation of the dissociating moieties, the clearly defined surface leading to ground state CO<sub>2</sub> indicates that an energetically low-lying exit channel must exist, with barriers of about 5-6 kcal mol<sup>-1</sup> for the CH<sub>3</sub>C(O)O<sup>•</sup> radical, and 3-4 kcal mol<sup>-1</sup> for the CH<sub>3</sub>CH<sub>2</sub>C(O)O<sup>•</sup> reactant. With such low

barriers, then, and considering the very high pre-exponential factor for decomposition, it seems unlikely that other processes will be able to compete with CO<sub>2</sub> elimination.

### 3.3 Hydroxy substituents (-OH)

Similar to oxo-substitution, hydroxy substituents are readily formed in the partial oxidation of hydrocarbons in the atmosphere, e.g. by OH radical addition on unsaturated compounds, or H-shift reactions in alkoxy radicals.  $\alpha$ -Hydroxy-substituents lead to carboxylic acids after decomposition, while  $\beta$ -OH substituents form hydroxy-substituted alkyl radicals that usually react with O<sub>2</sub>, forming carbonyl compounds and HO<sub>2</sub>. Hydroxy substitution is very effective in lowering the barrier height for decomposition, both in the  $\alpha$ - and  $\beta$ -position of the alkoxy radical.<sup>1,18</sup> These reactants form internal hydrogen bonds, which remain intact in the decomposition transition state and the hydrogen-bonded product complex even for  $\beta$ -OH alkoxy radicals,<sup>19,20</sup> such that the H-bond in itself does not alter the barrier for decomposition appreciably. However, if multiple hydroxy substituents are present near the breaking bond, it is unlikely that the necessary changes in the geometry of the two fragments, i.e. the hybridisation change from sp<sup>3</sup> to sp<sup>2</sup> for two of the carbons involved, will allow all of the hydrogen bonds to remain of identical strength in the transition state as in the parent molecule. Due to lack of data on this aspect, we do not account for such multiple H-bonding at this time.

### 3.4 Alkoxy substituents (-OR)

Alkoxy radicals with alkoxy substituents are found in the degradation of ethers and esters. Radicals with alkoxy substituents can also be formed in the addition of alkoxy radicals onto a double bond, including intramolecular ring closure in unsaturated alkoxy radicals shown to be important in atmospheric chemistry.<sup>21</sup> The alkyl-group within the -OR alkoxy substituents examined does not seem to affect the barrier appreciably, so for the purpose of this SAR all such alkyl groups are lumped into a single substituent class. Experimental evidence indicates<sup>22,23,24,25</sup> that  $\alpha$ -alkoxy alkoxy radicals, >C(O<sup>•</sup>)-OR, can also eliminate the -OR alkoxy substituent as a free radical. In the current SAR, we do not examine such O-C(O<sup>•</sup>) scission reactions.

### 3.4 Hydroperoxy and alkylperoxy substituents (-OOH and -OOR)

The reaction of alkylperoxy radicals RO<sub>2</sub> with HO<sub>2</sub> usually yields hydroperoxides, ROOH. Similarly, the RO<sub>2</sub> + R'O<sub>2</sub> reactions can produce peroxides, ROOR', with a (low) yield depending on the specific peroxy radicals examined. These compounds have

low volatilities and are expected to contribute to SOA formation. Ring closure reactions in large, unsaturated alkylperoxy radicals have been characterized,<sup>21</sup> yielding  $\beta$ -peroxide alkyl radicals. We have shown<sup>26</sup> that decomposition of an alkoxy radical with a  $\beta$ -(hydro)peroxy substituent,  $>C(OOR)-C(O^\bullet)<$ , leads to  $\alpha$ -(hydro)peroxy-substituted alkyl radicals which decompose spontaneously to a carbonyl compound and an  $^\bullet OH/^\bullet OR$  fragment:  $>C^\bullet(OOR) \rightarrow >C=O + ^\bullet OR$ . The observable products of such an alkoxy radical decomposition are then two carbonyl compounds and an O-centered radical fragment.

### 3.5 Nitrogen-oxygen-bearing substituents (-NO, -NO<sub>2</sub>, -ONO, -ONO<sub>2</sub>)

In addition to direct emission of compounds with nitrogen-oxygen-bearing substituents, such functionalities can also be formed in the atmosphere by reactions of alkyl, alkoxy and alkylperoxy radicals with NO, NO<sub>2</sub>, and NO<sub>3</sub> radicals, or the reaction of unsaturated species with NO<sub>3</sub> radicals as shown to be important in the night-time chemistry. The impact of N<sub>x</sub>O<sub>y</sub>-substituents on the chemical processing of organics in the atmosphere is largely unknown. The total contribution of such compounds is comparatively small, but (re)generation of NO<sub>x</sub> from such compounds might affect the nitrogen cycle. We examine here the impact of -NO, -NO<sub>2</sub>, -ONO, and -ONO<sub>2</sub> substituents; for many of these compounds, no systematic study on their influence on alkoxy decomposition has been performed earlier.

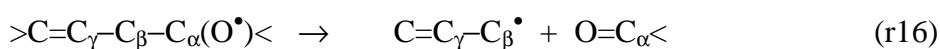
For  $\beta$ -nitroxy-substituted alkoxy radicals, readily formed in the NO<sub>3</sub>-initiated oxidation of alkenes, one of the decomposition products is an  $\alpha$ -nitroxy alkyl radical:  $C_\alpha H_2(O^\bullet)-C_\beta H_2 ONO_2 \rightarrow H_2 CO + ^\bullet C_\beta H_2 ONO_2$ . We have shown earlier<sup>27</sup> that these  $>C^\bullet ONO_2$  product radicals decompose spontaneously to a carbonyl compound  $>C=O + NO_2$ . Also, according to our calculations,  $\alpha$ -nitroso alkoxy radicals,  $-C(O^\bullet)(NO)-$  are thermally unstable, and dissociate with a negligible barrier to a carbonyl compound  $>C=O$  and NO.

### 3.6 Unsaturated compounds

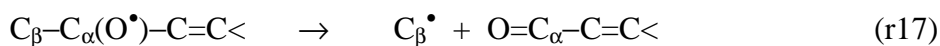
The presence of a double bond can greatly increase the stability of a radical by delocalisation of the unpaired electron by allyl-type resonance. Conversely, the presence of a double bond can also hamper product radical formation, as the formation of vinyl radicals is energetically unfavorable. Given that a wide variety of poly-unsaturated compounds are emitted into the troposphere in vast quantities, including isoprene and

monoterpenes, many alkoxy radicals formed in the atmosphere have an unsaturated functionality within the carbon chain. The impact of a double bond on the decomposition process is specific to its position relative to the  $\alpha$ - and  $\beta$ -carbons. Ignoring the unlikely possibility of breaking the double bond itself, four specific cases can be distinguished. The code used for notating such substitutions in the tables is also defined here.

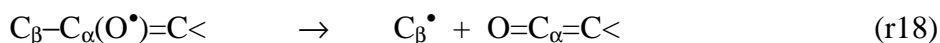
a) A double bond on the  $\gamma$ -carbon (notation  $\beta$ -C=C) allows for allyl-type resonance stabilization of the product alkyl radical:  $C=C-C^{\bullet} \leftrightarrow \bullet C-C=C$ . This increases the exoergicity of the decomposition reaction and lowers the barrier to reaction.



b) A double bond adjacent to the  $\alpha$ -carbon (notation  $\alpha$ -C=C) leads to a conjugated  $\pi$ -system after decomposition, stabilizing the product carbonyl compound.



c) A double bond directly on the  $\alpha$ -carbon (notation  $\alpha=C$ ) correspond to a vinoxy-type reactant radical,  $\bullet O-C=C \leftrightarrow O=C-C^{\bullet}$ , where only about 20% of the radical character is located on the oxygen atom. Breaking an adjacent C-C bond involves breaking a relatively strong alkenyl bond, and leads to a ketene, eliminating the resonance stabilization:



In atmospheric conditions, it is unlikely for such a compound to undergo C-C bond scission, as the most dominant resonance structure,  $O=C-C^{\bullet}$ , will readily react with  $O_2$  to form a 2-oxo-peroxy radical.

d) If the  $\beta$ -carbon is doubly bonded (notation  $\beta=C$ ), decomposition of the alkoxy radical involves breaking a alkenyl bond, leading to a vinyl radical after decomposition.



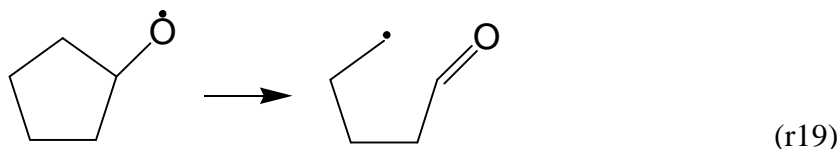
In the first two cases, the presence of the double bond increases the reaction exoergicity, and is expected to increase the rate of decomposition. The latter two cases, however, both involve unfavorable changes to the bonding, leading to more endothermic decomposition reactions; for these, the barrier to decomposition is expected to increase. In compounds where resonance stabilization occurs, the substitution on all of the resonance radical sites affects the stability to some extent, i.e. a difference in resonance

stabilization energy is expected between e.g. two primary (terminal) radical resonance sites, versus a secondary-tertiary site resonance. For the OH-addition on conjugated alkenes, we showed that this difference in substitution can affect the rate coefficient appreciably.<sup>28</sup>

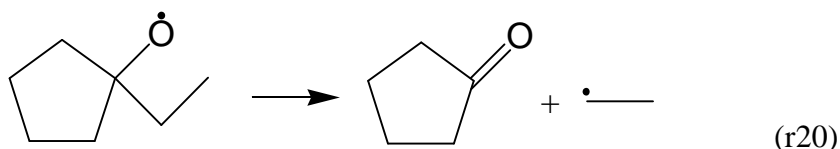
In this SAR, we do not account for the substitution-dependent resonance, lumping all compounds in a single reaction class.

### 3.7 Cyclic compounds

Cyclic compounds with rings of 5 or less carbons contain a sizable amount of ring strain. Logically, the release of this ring strain upon ring breaking will lower the barrier to decomposition.



Ring breaking reactions for smaller rings therefore needs specific consideration. Note that rings that are strain-free, e.g. cyclohexoxy, have barriers that are very close to non-cyclic compounds of similar substitution. The presence of a ring can also affect bond breaking transition states in which the ring remains intact, i.e. decompositions where either the  $\alpha$ - or  $\beta$ -carbon are in a ring structure that remains intact in the decomposition.



In such cases, one of the carbons involved in the ring will prefer to change its hybridization from  $sp^3$  to  $sp^2$ , either to accommodate the newly formed C=O double bond, or to assume the planar geometry preferred for the  $>C^{\bullet}$  carbon product radical site. This geometry change can increase or decrease the ring strain in the product, depending on the characteristics of the ring structure. Even though polycyclic compounds with fused rings constitute a large fraction of the hydrocarbons emitted in the troposphere, we only examine mono-cyclic structures at this point.

## Statistical analysis of the fitting procedure

As an example, we give the output of the statistical fitting procedure for alkyl-substitution (first stage of the multi-step activity determination).

### Input data:

```
print(sardata)
      Molecule      Eb naalkyl nbalkyl
1      3-Me-2-butoxyl  8.317322      1      2
2      2-Me-2-butoxyl  9.742640      2      1
3      2-Me-2-pentoxyl  9.933509      2      1
4          2-pentoxyl 11.544673      1      1
5          2-butoxyl 11.557568      1      1
6      2-Me-1-propoxyl 11.644789      0      2
7          3-pentoxyl 12.186097      1      1
8      2-3-diMe-2-butoxyl 13.401174      2      0
9      2-3-3-triMe-2-butoxyl 13.475034      2      0
10         2-Me-2-pentoxyl 13.682696      2      0
11         2-Me-2-butoxyl 13.801332      2      0
12         2-Me-2-propoxy 13.945248      2      0
13             1-pentoxyl 14.821687      0      1
14             1-propoxy 14.853901      0      1
15             1-butoxyl 14.959947      0      1
16      3-3-diMe-2-butoxyl 15.075041      1      0
17             2-propoxy 15.135122      1      0
18         3-Me-2-butoxyl 15.383378      1      0
19             2-pentoxyl 15.389745      1      0
20             2-butoxyl 15.517186      1      0
```

### Fitting summary:

```
Call:
lm(formula = Eb ~ 1 + naalkyl + nbalkyl, data = subsetdata)

Residuals:
    Min       1Q   Median       3Q      Max
-0.64779 -0.29228  0.02535  0.35229  0.63545

Coefficients:
            Estimate Std. Error t value Pr(>|t|)
(Intercept)  17.9418      0.2656   67.56 < 2e-16 ***
naalkyl       -2.3160      0.1559  -14.86 3.59e-11 ***
nbalkyl       -3.4334      0.1706  -20.12 2.72e-13 ***
---
Signif. codes:  0 '***' 0.001 '**' 0.01 '*' 0.05 '.' 0.1 ' ' 1

Residual standard error: 0.4389 on 17 degrees of freedom
Multiple R-squared:  0.9625,    Adjusted R-squared:  0.958
F-statistic: 218 on 2 and 17 DF, p-value: 7.633e-13

AIC: 28.57168
```

Diagnostic plots:

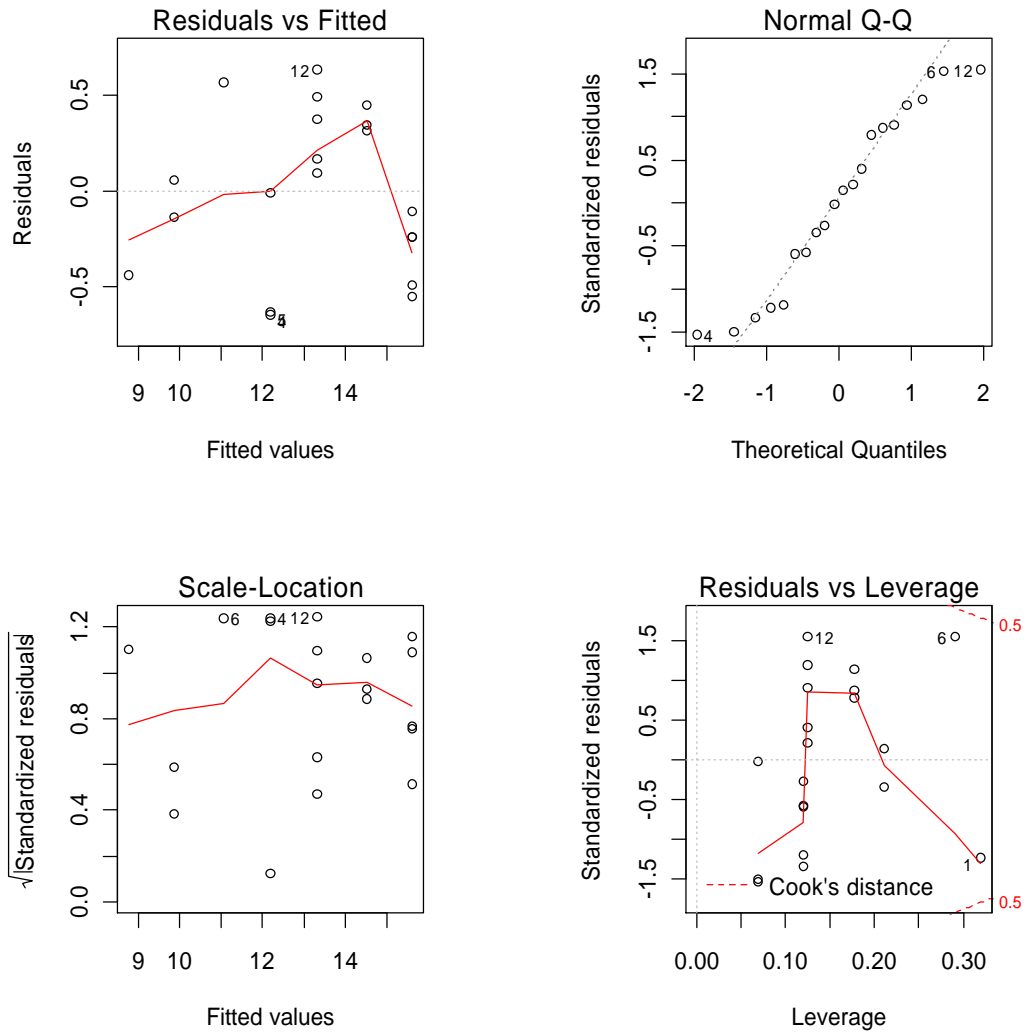


**Fig. SI-6:** Diagnostic plots of the linear fitting.

## SAR parameters in $\text{kJ mol}^{-1}$

**Table SI-6** Alkoxy decomposition SAR activities  $F_s$  ( $\text{kJ mol}^{-1}$ ) for substituents on the  $\alpha$ - or  $\beta$ -carbon, for  $E(\text{CH}_3\text{CH}_2\text{O}^\bullet) = 75 \text{ kJ mol}^{-1}$ .

Substituent	$F_s$	Substituent	$F_s$
$\alpha$ -alkyl	-10 <sup>a</sup>	$\beta$ -alkyl	-14
$\alpha$ =O	-53	$\beta$ =O	-36
$\alpha$ -OH	-37	$\beta$ -OH	-31
$\alpha$ -OR (R=alkyl)	-39	$\beta$ -OR (R=alkyl)	-38
$\alpha$ -OOH	-37	$\beta$ -OOH <sup>c</sup>	-39
$\alpha$ -OOR (R=alkyl)	-27	$\beta$ -OOR (R=alkyl) <sup>c</sup>	-30
$\alpha$ -NO	N/A <sup>b</sup>	$\beta$ -NO	-67
$\alpha$ -NO <sub>2</sub>	-9	$\beta$ -NO <sub>2</sub>	+2
$\alpha$ -ONO	-18	$\beta$ -ONO	-25
$\alpha$ -ONO <sub>2</sub>	-16	$\beta$ -ONO <sub>2</sub> <sup>d</sup>	-12
$\alpha$ =C	+90	$\beta$ =C	+21
$\alpha$ -C=C	-20	$\beta$ -C=C	-40

<sup>a</sup> If only 1 substituent is present on the  $\alpha$ -carbon of the form  $-\text{CHO}$ ,  $-\text{CH}_2\text{OR}$ ,  $-\text{CH}_2\text{OOH}$ , or  $-\text{CH}_2\text{OOR}$  (R=alkyl), use  $F_s = -3$ .

<sup>b</sup> Compounds of the form  $>\text{C}(\text{O}^\bullet)-\text{NO}$  spontaneously decompose to  $>\text{C}=\text{O} + \bullet\text{NO}$

<sup>c</sup> Product radicals of the form  $>\text{C}^\bullet\text{OOH}$  and  $>\text{C}^\bullet\text{OOR}$  spontaneously decompose to  $>\text{C}=\text{O} + \bullet\text{OH}$  or  $\bullet\text{OR}$ .<sup>26</sup>

<sup>d</sup> Product radicals of the form  $>\text{C}^\bullet\text{ONO}_2$  spontaneously decompose to  $>\text{C}=\text{O} + \bullet\text{NO}_2$ .<sup>27</sup>

**Table SI-7** SAR activities  $F_s$  (kJ mol<sup>-1</sup>) for alkoxy radical decomposition where C<sub>α</sub> or C<sub>β</sub> are member of a ring structure, and where decomposition retains this ring structure. The activities include the contribution of the hydrocarbon chain constituting the ring.

Substituent		$F_s$
α-c-prop	C <sub>α</sub> in 3-membered ring	<i>N/A</i> <sup>a</sup>
α-c-but	C <sub>α</sub> in 4-membered ring	-8
α-c-pent	C <sub>α</sub> in 5-membered ring	-9
α-c-hex	C <sub>α</sub> in 6-membered ring	-9
β-c-prop	C <sub>β</sub> in 3-membered ring	+10
β-c-but	C <sub>β</sub> in 4-membered ring	-18
β-c-pent	C <sub>β</sub> in 5-membered ring	-29
β-c-hex	C <sub>β</sub> in 6-membered ring	-29

<sup>a</sup> The 3-membered ring in substituted cyclopropoxy breaks without barrier.

**Table SI-8** SAR activities  $F_s$  (kJ mol<sup>-1</sup>) for ring opening, including the contribution of the hydrocarbon chain constituting the ring.

Ring size	$F_s$
3-membered ring	-103
4-membered ring	-71
5-membered ring	-36
6-membered ring	-26

## References

---

- <sup>1</sup> J. Peeters, G. Fantechi and L. Vereecken, *J. Atmos. Chem.*, 2004, **48**, 59.
- <sup>2</sup> A.D. Becke, *J. Chem. Phys.*, 1992, **97**, 9173.
- <sup>3</sup> A. Lee, W. Yang, and R.G. Parr, *Phys. Rev. B*, 1988, **37**, 785.
- <sup>4</sup> Y. Zhao, B. J. Lynch, and D. G. Truhlar, *J. Phys. Chem. A*, 2004, **104**, 2715.
- <sup>5</sup> B. J. Lynch, P. L. Fast, M. Harris, and D. G. Truhlar, *J. Phys. Chem. A*, 2000, **104**, 4811.
- <sup>6</sup> Y. Zhao, N. González-García, and D. G. Truhlar, D. G., *J. Phys. Chem. A*, 2005, **109**, 2012.
- <sup>7</sup> J. A. Montgomery Jr., M. J. Frisch, J. W. Ochterski, and G. A. Petersson, *J. Chem. Phys.* 2000, **112**, 6532.
- <sup>8</sup> M. J. Frisch, *et al.*, GAUSSIAN-98, Rev. A.9, Gaussian, Inc., Pittsburgh PA, 1998.
- <sup>9</sup> M. J. Frisch, *et al.*, GAUSSIAN-03, Rev. D.02, Gaussian, Inc., Wallingford CT, 2004
- <sup>10</sup> J. J. Orlando, G. S. Tyndall, L. Vereecken, and J. Peeters, *J. Phys. Chem. A* 2000, **104**, 11578.
- <sup>11</sup> H. Somnitz, and R. Zellner, *Phys. Chem. Chem. Phys.* 2000, **2**, 4319.
- <sup>12</sup> R. Méreau, M.-T. Rayez, J.-C. Rayez, and P. C. Hiberty, *Phys. Chem. Chem. Phys.* 2001, **3**, 3656.
- <sup>13</sup> H. Somnitz and R. Zellner, *Phys. Chem. Chem. Phys.*, 2000, **2**, 1907.
- <sup>14</sup> R. Karunanandan, D. Hölscher, T. J. Dillon, A. Horowitz, J. N. Crowley, L. Vereecken, and J. Peeters, *J. Phys. Chem. A* 2007, **111**, 897.
- <sup>15</sup> D. Feller, D. A. Dixon, and J. S. Francisco, *J. Phys. Chem. A* 2003, **107**, 1604.
- <sup>16</sup> W. Sun, and M. Saeys, *J. Phys. Chem. A* 2008, **112**, 6918.
- <sup>17</sup> D.-Y. Hwang, and A. M. Mebel, *Chem. Phys.* 2000, **256**, 169.
- <sup>18</sup> J. J. Orlando, G. S. Tyndall, M. Bilde, C. Ferronato, T. J. Wallington, L. Vereecken, and J. Peeters, *J. Phys. Chem. A* 1998, **102**, 8116.
- <sup>19</sup> L. Vereecken, and J. Peeters, *J. Phys. Chem. A*, 1999, **103**, 1768.
- <sup>20</sup> L. Vereecken, J. Peeters, J.J. Orlando, G.S. Tyndall, and C. Ferronato, *J. Phys. Chem. A*, 1999, **103**, 4693.
- <sup>21</sup> L. Vereecken, and J. Peeters, *J. Phys. Chem. A*, 2004, **108**, 5197
- <sup>22</sup> R. Atkinson, *Atmos. Environ.*, 2007, **41**, 8468.
- <sup>23</sup> T. J. Wallington, and S. M. Japar, *Environ. Science. Techn.*, 1991, **25**, 410.
- <sup>24</sup> D. F. Smith, T. E. Kleindiest, E. E. Hudgens, C. D. McIver, and J. J. Bufalini, *Int. J. Chem. Kinet.*, 1992, **24**, 199.
- <sup>25</sup> S. M. Aschmann, and R. Atkinson, *Int. J. Chem. Kinet.*, 1999, **31**, 501.
- <sup>26</sup> L. Vereecken, T. L. Nguyen, I. Hermans, and J. Peeters, *Chem. Phys. Lett.*, 2004, **393**, 432.
- <sup>27</sup> L. Vereecken, *Chem. Phys. Lett.*, 2008, **466**, 127.
- <sup>28</sup> J. Peeters, W. Boullart, V. Pultau, S. Vandenberk, and L. Vereecken, *J. Phys. Chem. A* 2007, **111**, 1618.